

# lncRNA/mRNA profiling of endometriosis rat uterine tissues during the implantation window

HAN CAI, XINXIN ZHU, ZHANFEI LI, YAPEI ZHU and JINGHE LANG

Department of Obstetrics and Gynecology, Peking Union Medical College Hospital, Beijing 100005, P.R. China

Received April 23, 2019; Accepted September 17, 2019

DOI: 10.3892/ijmm.2019.4370

**Abstract.** Endometriosis is associated with changes in long non-coding RNA (lncRNA) and mRNA expression, but the exact changes during the implantation window are unknown. Therefore, this study aimed to explore the lncRNA and mRNA expression profiles in the uterus of rats with endometriosis during the implantation window. A total of 35 non-pregnant female rats were randomized to the endometriosis (n=13), adipose tissue control (n=8) and blank control (n=14) groups. On the 5th day of pregnancy, the rats were sacrificed to obtain uterine tissues. lncRNA and mRNA were analyzed using gene chips. A total of five differentially expressed lncRNA and four mRNA were validated by reverse transcription-quantitative (RT-q)PCR. Immunohistochemistry and western blotting were used to determine the expression of the ADAM metallopeptidase with thrombospondin type 1 motif 7 (Adamts7), tumor protein p53 (Tp53), distal-less homeobox 3 (Dlx3) and pyrimidinergic receptor P2Y6 (P2ry6) proteins. There were 115 upregulated lncRNAs, 51 downregulated lncRNAs, 97 upregulated mRNAs and 85 downregulated mRNAs in the endometriosis group. RT-qPCR confirmed the trends for five lncRNAs and four mRNAs (Adamts7, Tp53, Dlx3 and P2ry6). The relative protein expression levels of Adamts7, P2ry6, Dlx3 and TP53 were significantly different in the endometriosis group ( $P < 0.05$  vs. controls). Bioinformatics predicted the co-expression relationship of the selected five lncRNA and four mRNA. Gene ontology and the Kyoto Encyclopedia of Genes and Genomes predicted that Adamts7, P2ry6, Dlx3 and TP53 were involved in endometriosis-related inflammation and reproductive pathways. In conclusion, the changes in

the expression of lncRNAs, mRNAs and proteins (Adamts7, P2ry6, Dlx3 and TP53) may possibly affect endometrial receptivity in rats with endometriosis during the implantation window, probably resulting in implantation failure of the embryo.

## Introduction

A total of ~2-10% of women suffer from endometriosis and 50% of them have infertility issues (1), mainly of the estrogen-dependent inflammatory type (2,3). The glandular epithelium and basement membrane of human endometrium undergo periodic changes in gene expression, which must be synchronized to allow the opening of the implantation window. Any abnormality in gene expression could lead to a small or absent window. The abnormal inflammatory state caused by endometriosis impairs endometrial receptivity (4).

Long non-coding RNAs (lncRNAs) are non-coding RNAs with a length of >200 nucleotides and a wide range of biological functions. A number of studies reported various lncRNAs to be associated with endometriosis and compromised fertility (5-8). A total of two genome-wide screening studies showed that there were 1,000 lncRNA (9) and 1,300 mRNA (10) transcripts that were abnormally expressed between eutopic and ectopic endometrial tissues of patients with endometriosis. Another study revealed that 1,277 lncRNAs and 1,216 mRNAs were differentially expressed between the eutopic and ectopic endometrium of patients with endometriosis during the late secretory phase (11). Taken together, these studies highlight the important regulatory roles of lncRNAs in endometriosis.

In the present study, the difficulty of obtaining clinical specimens of the endometrium during the implantation window was taken into consideration. Therefore, autologous endometrial transplantation was used to establish a model of endometriosis in Sprague-Dawley rats. The present study aimed to determine the changes in lncRNAs and mRNAs in the uterine tissues of those rats during the implantation window, using microarrays. The present study hypothesized that the abnormalities in lncRNA and mRNA profiles have significant effects on the implantation ability of uterine tissues in rats with endometriosis during the implantation window, which could be an important cause of endometrial receptivity impairment in endometriosis.

*Correspondence to:* Dr Jinghe Lang, Department of Obstetrics and Gynecology, Peking Union Medical College Hospital, 1 Shuaifuyuan, Dongcheng, Beijing 100005, P.R. China  
E-mail: langjinghe1555@sina.com

**Abbreviations:** cDNA, complementary DNA; H&E, hematoxylin and eosin; lncRNA, long non-coding RNA; PCC, Pearson's correlation coefficient

**Key words:** endometriosis, infertility, long non-coding RNA, mRNA

## Materials and methods

**Ethics statement.** The present study was approved by the Experimental Animal Center of the Peking Union Medical College Hospital and Chinese Academy of Medical Sciences (permit no. XHDW-2016-000). All experiments were performed in accordance with the principles of experimental animal management and protection. The rats were humanely cared for and sacrificed to prevent suffering.

**Experimental animals and collection of specimens.** Clean, sexually mature and non-pregnant Sprague-Dawley female (n=35) and male (n=10) rats were selected. The age of the female rats was 60-70 days and their weight was 200±10 g. The weight of the male rats was 380±10 g (age, 60-70 days). All rats were purchased from Beijing Vital River Laboratory Animal Technology Co., Ltd., and they were kept in the specific pathogen-free facility of the Laboratory Animal Center of Peking Union Medical College Hospital. Room temperature was 20-25°C and relative humidity was 45-60%. The rats were housed five per cage. All rats were kept under 14-h light/10-h dark cycle. They received sterilized feed and water *ad libitum*. They were adaptively fed for 2-3 days before experiments. The vaginal smear method was used to determine the estrous cycle of each female rat, which was usually 4-5 days.

The 35 female rats were divided into three groups: Endometriosis group (n=13), adipose tissue control group (n=8) and blank control group (n=14). After the observation of three estrous cycles, the autologous transendocardial transplantation method described by Vernon and Wilson (12) was performed, but with slight improvements. In the endometriosis group, a segment of autologous uterine tissue was collected and transplanted onto the abdominal wall in the fourth estrus cycle. Pentobarbital sodium (5%, 50 mg/kg, i.p.) was used for anesthesia. The rats were placed in a supine position and the abdominal skin was prepared. A longitudinal abdominal incision (5 cm) was made to open the abdominal cavity and to find the Y-shaped uterus. The left uterine horn was lifted and uterine tissue (1 cm) was collected and quickly placed in a culture dish with saline water. The extra adipose tissues outside the serous layer were removed. A longitudinal incision of the uterine cavity was made and two pieces (5x5 mm) were sutured on both sides of the abdominal wall at sites rich in blood vessels. Then the abdominal incision was sutured layer by layer.

In the adipose tissue control group, eight female rats were randomly selected. They underwent the same surgery as in the endometriosis group, but the left uterine horn was ligated and two pieces of adipose tissues (5x5 mm) were collected from the abdomen and sutured onto both sides of the abdominal wall. In the blank control group, no surgery was performed.

A total of 28 days after operating, the rats in the endometriosis and adipose tissue groups were re-operated to observe the growth, invasion and adhesion of the transplanted endometrium. Growth of ectopic endometrium (the transplanted tissues were 5x5 mm), tissue edema (as a sign of inflammation) and vesicle formation were observed by the naked eye. The models were considered successful if the transplanted endometrium has grown by at least 2-fold. The model success rate was calculated as the number of successful models divided by the

total number of animals that underwent modeling. The scoring criteria of the ectopic uterine tissue growth were: Score 0, no epithelium; score 1, poorly preserved epithelium; score 2, moderately preserved epithelium; and score 3, well preserved epithelium (13,14). The abdominal incision was sutured layer by layer. All rats survived and were prepared for mating.

A total of 10 male rats were kept in different cages. The female rats were placed in the cages with one male rat at 18:00 every night and a tray was placed under each cage. At 8:00-9:00 the next morning, the trays were checked for vaginal plugs and vaginal smear examinations were carried out. If a vaginal plug and sperm were observed under the microscope at the same time, it was considered to be the 1st day of pregnancy (D1) (15), and mating was not conducted anymore. On the 5th day of pregnancy (D5) [i.e., during the short implanting window; implantation occurs on day 5 in rats (15)], female rats were sacrificed to collect the uterine tissues. The tissues were divided into two parts. One part was put in 10% formalin at 4°C for at least 24 h for subsequent hematoxylin and eosin (H&E) staining and immunohistochemistry. The other part was quickly put into liquid nitrogen at -80°C for gene chip analysis and reverse transcription-quantitative (RT-q)PCR. All experiments were performed using the samples from the same rats in each group.

**RNA extraction.** According to the manufacturer's protocol, TRIzol (Invitrogen; Thermo Fisher Scientific, Inc.) was used to extract the total RNA from the uterine tissues (100 mg). RNA was purified using the mirVana miRNA Isolation kit (Ambion; Thermo Fisher Scientific, Inc.). RNA concentration and purity were determined by spectrophotometry (NanoDrop ND-1000; Thermo Fisher Scientific, Inc.) to measure optical density at 260/280 nm. The RNA 6000 Nano Lab-on-a-Chip kit and the Bioanalyzer 2100 (Agilent Technologies, Inc.) were used and RNA integrity was verified by electrophoresis on formaldehyde (1%) gels. The tissues with RNA integrity >6 were selected for the subsequent experiments.

**Microarray imaging and data analysis.** Complementary(c) DNA was synthesized from 5 µl total RNA. The GeeDom® biochip (CapitalBio Corp.) labeling kit was used. The Nucleospin® Extract II kit (Macherey-Nagel, GmbH) was used to purify the labeled products. The rat lncRNA+mRNA Array V1.0 (8x60K format, the sequence included 4,974 control probes; Agilent Technologies, Inc.) was used for hybridization. The probes in each sequence represented 22,020 rat lncRNAs and 30,254 rat mRNAs. These lncRNA and mRNA probes sequences referred to multiple databases including NCBI RefSeq (<https://www.ncbi.nlm.nih.gov/refseq/>), Ensembl (<http://www.ensembl.org/index.html>), UCSC genome browser (<http://genome.ucsc.edu/>), NONCODE V4.0 (<http://www.noncode.org>) and UCR (<https://users.soe.ucsc.edu/~jill/ultra.html>) (16). Each RNA is detected by the probe at least 1-2 times and each microarray includes 4,974 probes.

After hybridization, the chip was washed in the GeeDom® Slide Washer 8. The Agilent chip scanner (G2565CA) was used to scan the chip. The Agilent Feature Extraction (v10.7) software (Agilent Technologies, Inc.) was used to analyze the images. The GeneSpring software V13.0 (Agilent Technologies, Inc.) was used for the summary, standardization and quality

control of chip data. Values of  $\geq 2$  and  $\leq -2$  fold-change, as well as  $P < 0.05$  were used for screening for differentially expressed genes. CLUSTER 3.0 software (Stanford University) with data adjustment functions was used to perform the log<sub>2</sub> conversion and median calculation of chip data. Finally, the Java Treeview v1.8 (Stanford University School of Medicine) was used for cluster analysis. The samples were tested in triplicates.

**RT-qPCR validation of differentially expressed lncRNAs and mRNAs.** The criteria for selecting the candidate differentially expressed genes for validation were: i) Fold-change was  $\geq 2$ ; ii) the biological repeat of each group was  $\geq 3$ ; and iii)  $P \leq 0.05$ . For an upregulated gene, the number of samples with the detected flag of the experimental group was required to be  $>60\%$  of the total number of samples in the group. For a downregulated gene, the number of samples with the detected flag of the control group was required to be  $>60\%$  of the total number of samples in the group.

Therefore, according to bioinformatics, the relationship between the targeted regulation of the selected five lncRNAs and the mRNA microarray results (abnormal expression folds in the endometriosis group and the blank control group) were selected for four mRNAs [ADAM metalloproteinase with thrombospondin type 1 motif 7 (Adamts7), tumor protein p53 (Tp53), distal-less homeobox 3 (Dlx3) and pyrimidinergic receptor P2Y6 (P2ry6)] for qPCR validation.

The primers are shown in Table I. The FastQuant RT kit [Tiangen Biotech (Beijing) Co., Ltd.] was used for the reverse transcription of total RNA: 1  $\mu$ g total RNA and 20  $\mu$ l reaction system (10X Fast-RT Buffer 2  $\mu$ l, FQ-RT Primer Mix 2  $\mu$ l, RT Enzyme Mix 1  $\mu$ l, RNase-Free water 5 and 10  $\mu$ l buffer) were kept at 42°C for 15 min, 95°C for 3 min, cooled on ice and reverse transcribed. The same amount of RNA was used for all samples. The qPCR reaction system Power SYBR®-Green PCR Master Mix (Applied Biosystems; Thermo Fisher Scientific, Inc.; 10  $\mu$ l) containing Power SYBR®-Green PCR Master Mix (2X) 5  $\mu$ l, cDNA sample 0.5  $\mu$ l, forward primer (10  $\mu$ M, 0.25  $\mu$ l), reverse primer (10  $\mu$ M, 0.25  $\mu$ l) and nuclease-free water (4  $\mu$ l) were used in a MicroAmp Optical 96-Well Reaction Plate (Applied Biosystems; Thermo Fisher Scientific, Inc.). Denaturation was carried out at 95°C for 10 min in a QuantStudio™ 7 Flex RealTime PCR system (Applied Biosystems; Thermo Fisher Scientific, Inc.). Then, 40 cycles (95°C for 15 sec and 60°C for 1 min) and a final extension at 60°C for 10 min were performed, before climbing up to 95°C for melting curve analysis (temperature ramp of 2%). All RT-qPCR reactions were performed in triplicate. Electrophoresis (agarose gel, 2.0%) was used to detect the amplification specificity of the products. GAPDH was selected as the internal reference gene. Expression was measured using the  $2^{-\Delta\Delta C_q}$  method (17).

**Immunohistochemistry.** The SP method was used for immunohistochemistry (18). All specimens were fixed in neutral formalin (10%) for at least 24 h at room temperature, paraffin-embedded, sectioned (4  $\mu$ m) and dewaxed at 60°C overnight. Then, they were incubated in xylene for 45 min, hydrated in decreasing ethanol series and washed with distilled water for 5 min. After antigen retrieval, the slides were placed in PBS (pH 7.4), shaken and washed three times, 15 min each

time. The sections were placed in hydrogen peroxide (3%) to block endogenous peroxidase and incubated at room temperature for 25 min. The slides were placed in PBS (pH 7.4), shaken and washed three times, 15 min each time. Bovine serum albumin (3%) (Wuhan Servicebio Technology, Co., Ltd.) was added and incubated at room temperature for 30 min. After adding antibodies against Adamts7 (1:200; cat. no. 250456; Abbiotec, Inc.), P2ry6 (1:50; cat. no. GTX16829; GeneTex, Inc.), Dlx3 (1:100; cat. no. 27-520; ProSci, Inc.) and Tp53 (1:200; cat. no. 70-527; ProSci, Inc.), the slides were incubated at 4°C in a wet box for the night. The DAKO K5007 rat/rabbit secondary antibody (cat. no. K5007; ready-to-use preparation; Dako; Agilent Technologies, Inc.) was added and incubated at room temperature for 50 min. DAB coloration (cat. no. G1211; Wuhan Servicebio Technology, Co., Ltd.) was performed and stained with hematoxylin for 3 min at room temperature, before observation under a light microscope.

**Protein extraction and western blotting.** The frozen uterine tissues were homogenized in 5X protein loading buffer (G2013; Wuhan Servicebio Technology, Co., Ltd.) with phosphorylation protease inhibitor (G2007; Wuhan Servicebio Technology, Co., Ltd.), cooled on ice for 30 min and centrifuged at 13,000  $\times$  g for 10 min at 4°C. The supernatant was kept. The bicinchoninic kit (Wuhan Servicebio Technology, Co., Ltd.) was used to determine protein concentration. The protein solution [mixed 4:1 with 5X protein sample buffer (Wuhan Servicebio Technology, Co., Ltd.)] was boiled for 15 min and stored at -20°C. Proteins (30  $\mu$ g) were separated using 10% SDS-PAGE. Proteins were transferred to polyvinylidene difluoride membranes, which were blocked with 5% skimmed milk for 1 h at room temperature. The primary antibodies against P2ry6 (1:1,000), Adamts7 (1:1,000), Dlx3 (1:1,000) and Tp53 (1:1,000; cat. no. orb319621; Biorbyt, Ltd.) were incubated at 4°C overnight. The membranes were washed in TBST (Tween-20, 0.05%) three times at room temperature. The secondary antibody HRP-labeled goat anti rabbit (1:3,000; cat. no. GB23303; Wuhan Servicebio Technology, Co., Ltd.) was incubated at room temperature for 30 min. The membranes were washed in TBST and enhanced chemiluminescence reagents A and B (cat. no. G2014; Wuhan Servicebio Technology, Co., Ltd.) was carried out. Adobe Photoshop CS5 (Adobe Inc.) was used for image analysis.  $\beta$ -actin (1:3,000; cat. no. GB12001; Wuhan Servicebio Technology, Co., Ltd.) was selected as internal reference. Grey value analysis (alpha-EaseFC v4.0; Alpha Innotech Corporation) was carried out.

**Functional prediction of lncRNAs and co-expression with mRNAs.** As in a previous study (19), the Pearson correlation coefficient (PCC) between each abnormally expressed lncRNA and its co-expressed mRNA was calculated.  $PCC > 0.8$  or  $< 0.8$  and  $P < 0.01$  represented significantly related lncRNA/mRNA. The hypergeometric cumulative distribution function was used to conduct functional enrichment analysis for co-expressed mRNA. The function of lncRNA was predicted through gene ontology (GO) (<http://geneontology.org/>) and Kyoto Encyclopedia of Genes and Genomes (KEGG) pathway analysis (<http://www.genome.jp/kegg/>). On this basis, protein regulatory genes could be predicted using cis and trans (20,21). On the basis of the screening results of lncRNA and mRNA co-expression

Table I. Primers for reverse transcription-quantitative PCR.

Gene	Primers (5'-3')	Length
NONRATT003997	F: CAGGGTCGGGAACTTTGAGA R: CATCCAGTGTCCAGTGAGGG	22 bp
gil672027621 reflXR_592747.1l	F: CACGGAATGACAAGTGTGGG R: GGTGACTAATTGCCCCCGTA	104 bp
gil672045999 reflXR_591544.1l	F: CAGCTGGATCTGCTTTTCGGA R: AGGAGACCCCAGATAAGCCT	127 bp
NONRATT006252	F: ACATAGCATTGGGCCCTGTC R: TCTAAAAGTCTCAGAGCATTCTCAA	134 bp
gil672033904 reflXR_589853.1l	F: AAGGGTTGGGAAGACCATGAC R: GAGACTCCCTGCTCACTTACG	120 bp
Adamts7	F: TCAATTTCTGTGAGACGCTGC R: ATGGTGCGTGGGTTTATCGT	147 bp
Tp53	F: CCCACCGCCTGTAAGATTC R: GAGGGGTGGGGGATGGATA	110 bp
Dlx3	F: TCAATCTCAATGGGCTCGCA R: GGTACGCTCCATACTGTCCG	90 bp
P2ry6	F: GGTAGCTTGAGGCTGAGAGG R: TGACAGAAGTGTGTACGGCAT	126 bp
GAPDH	F: CCTCAAGATCATCAGCAAT R: CCATCCACAGTCTTCTGGGT	141 bp

Adamts7, ADAM metalloproteinase with thrombospondin type 1 motif 7; Tp53, tumor protein p53; Dlx3, distal-less homeobox 3; P2ry6, pyrimidine dinergic receptor P2Y6.

(correlation >0.99 or <-0.99 and  $P < 0.05$ ), cis-prediction looked for lncRNA-mRNA pair whose genomic location was within 10 kb and trans-prediction used Blat (<http://hgdownload.cse.ucsc.edu/admin/exe/>) to compare lncRNA and mRNA (3'UTR) sequences, and selected lncRNA-mRNA pair that had similar sequence and beyond 100 kb distance.

**Statistics analysis.** The tiff image data after hybrid scanning of the Gem<sup>®</sup>lncRNA+mRNA expression spectrum chip was preprocessed by the Feature Extraction software v10.7 (Agilent Technologies, Inc.). The GeneSpring GX software v13.0 (Agilent Technologies, Inc.) was used to calculate the differences of gene expression and statistical significance ( $P$ -value). Continuous data (such as the RT-qPCR data) were expressed as the mean  $\pm$  standard deviation and analyzed using analysis of variance with post hoc Tukey's test. The Fisher's exact test was used to analyze GO and KEGG data. The PCC was used to calculate the co-expression relationship between lncRNA and mRNA. SPSS 19.0 (IBM, Corp.) was used to conduct statistical analysis.  $P < 0.05$  was considered to indicate a statistically significant difference.

## Results

**Endometriosis modeling was successful.** On the 28th day after surgery, growth of ectopic endometrium of the transplanted tissues was 5x5 mm, tissue edema (a sign of inflammation) and vesicle formation (Fig. 1A) were observed. All rats in the endometriosis group were scored 3 with well-preserved

epithelium H&E staining showed that endometrial glands developed (Fig. 1B). In the adipose tissue control group, there was no change in the transplant (Fig. 1C) and H&E staining showed no endometrial glands (Fig. 1D). The abdominal walls of rats in the blank control group were normal. According to observation and H&E staining, the success rate of the endometrial transplantation modeling was 100%.

**Endometriosis is associated with differentially expressed lncRNAs.** Compared with the blank control group, the endometriosis model group showed 166 differentially expressed lncRNAs: 115 upregulated and 51 downregulated (fold-change  $> 2$ ) (Fig. 2A and Tables II and III).

In order to confirm the results of the gene chip analysis, three lncRNAs with upregulated expression (gil672027621|reflXR\_592747.1l, NONRATT006252 and gil672045999|reflXR\_591544.1l) and two lncRNAs with downregulated expression were selected for RT-qPCR validation. The expression trend and amplitude were consistent with the results of the gene chip analysis (Fig. 2B).

gil672066614|reflXR\_594547.1 (LOC103693263) was the most upregulated lncRNA [fold-change (FC)=5.35;  $P < 0.01$ ] (Tables II and III, and Fig. 3). NONRATT006252 (FC=3.42;  $P < 0.01$ ) and gil672045999|reflXR\_591544.1l (FC=2.88,  $P < 0.01$ ) were also significantly upregulated (Tables II and III, and Fig. 3).

NONRATT003997 was the most significantly downregulated (absolute FC=10.95;  $P < 0.01$ ) (Tables II and III, and Fig. 3). gil672033904|reflXR\_589853.1l was also significantly downregulated (absolute FC=5.79;  $P < 0.01$ ) (Tables II and III, and Fig. 3).



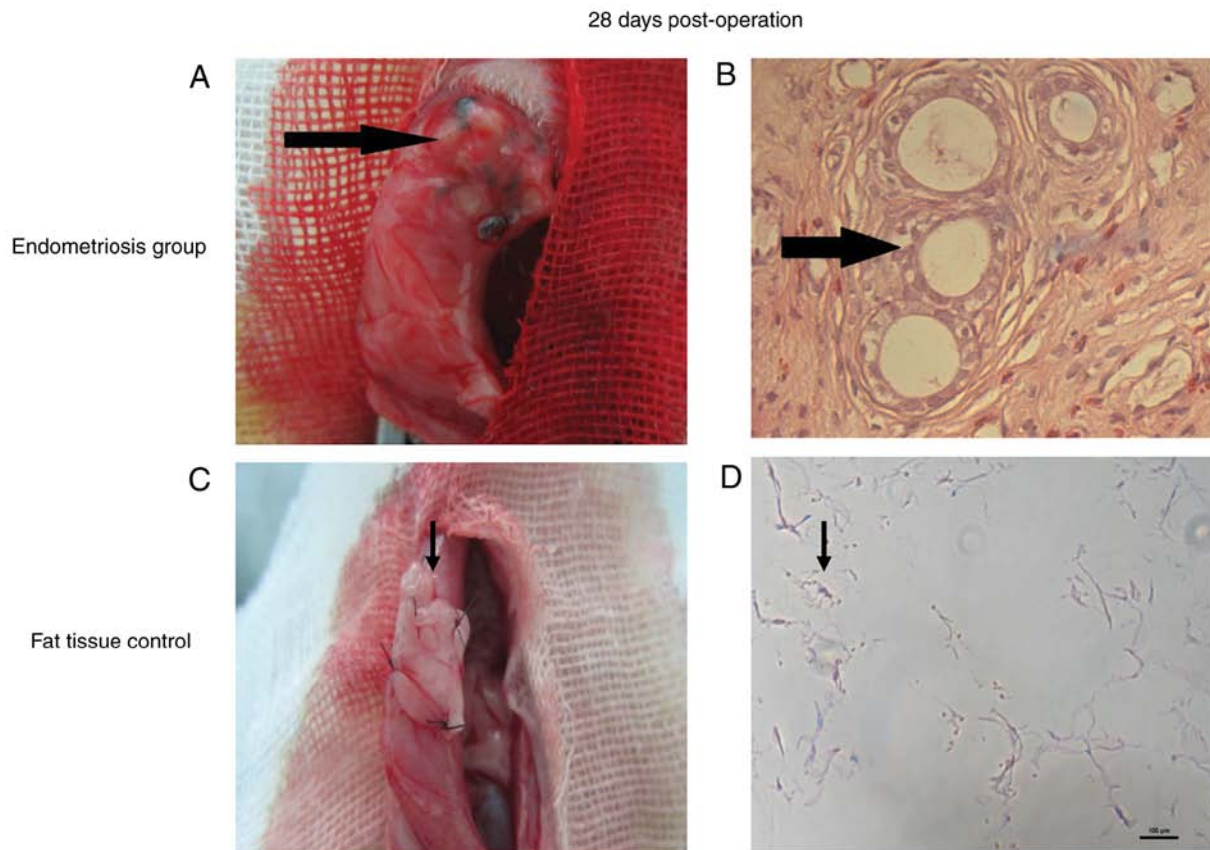


Figure 1. Endometriosis modeling is successful. (A) Volume growth, tissue edema and vesicle formation were observed in the endometriosis group. The arrow shows uterine tissue transplantation. (B) H&E staining showed that endometrial glands were developed in the endometriosis group (n=13). The arrow shows an endometrial gland. (C) In the adipose tissue control group (n=8), there was no change in the transplant. The arrow shows adipose tissue transplantation. (D) H&E staining showed no endometrial glands in the adipose tissue control group. Scale bar 100  $\mu$ m. The arrow show adipocytes. HE, hematoxylin and eosin.

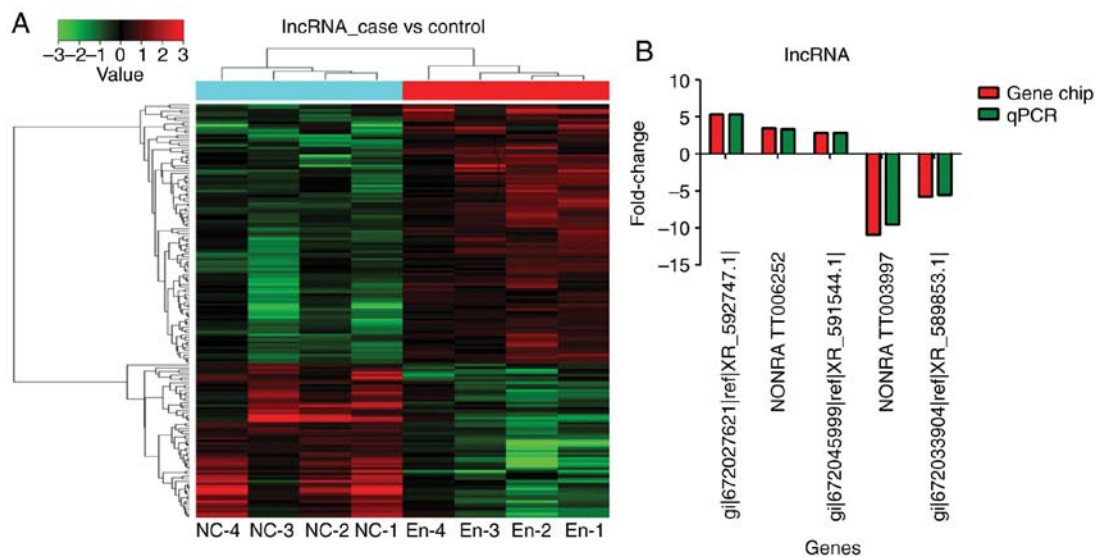


Figure 2. Compared with the blank control group (n=4), the endometriosis model group (n=4) shows 166 differentially expressed lncRNAs: 115 upregulated and 51 downregulated (fold-change >2). (A) Gene chip analysis. (B) Reverse transcription-quantitative PCR confirmation using five lncRNAs. The samples were tested in triplicates. Inc, long noncoding.

*Endometriosis is associated with differentially expressed mRNAs.* Overall, 182 mRNA transcripts were differentially expressed: 97 were upregulated and 85 were downregulated (fold-change >2) (Fig. 4A). According to bioinformatics, four mRNAs (Adams7,

Tp53, Dlx3 and P2ry6) were selected in the prediction of target regulation relationship with five lncRNAs and gene chip results. RT-qPCR validation showed that the expression of those mRNA was consistent with the gene chip analysis (Fig. 4B).

Table II. Top 20 upregulated lncRNA.

lncRNA (probe name)	FC (abs)	P-value	lncRNA (name)
gil672066614reflXR_594547.1l	5.34641	0.00327	LOC103693263
gil672076298lreflXR_595802.1l	4.895411	0.02629	LOC103693752
gil672079914lreflXR_360377.2l	4.506577	0.032437	LOC102548312
gil672036138lreflXR_590129.1l	3.46012	0.001325	LOC103691084
NONRATT018493	3.433898	0.008362	
NONRATT006252	3.42446	0.01579	
NONRATT020400	3.267124	0.019514	
NONRATT021467	3.102348	0.007103	
NONRATT025682	3.051757	0.00634	
NONRATT030954	3.017166	0.011163	
NONRATT011228	3.015996	0.002754	
NONRATT027460	2.978006	0.018386	
gil672045999lreflXR_591544.1l	2.87815	0.01452	LOC103691820
NONRATT012251	2.869275	0.01117	
NONRATT016194	2.819013	0.038048	
NONRATT010960	2.785293	0.022526	
gil672052626lreflXR_592505.1l	2.765093	0.006744	LOC103692352
gil672020316lreflXR_346989.2l	2.726432	0.001031	LOC102548283
gil672037438lreflXR_590367.1l	2.619791	0.00196	
NONRATT028550	2.596784	0.019415	

lnc, long noncoding; abs, absolute.

Adamts7 (A\_44\_P964460; FC=3.75,  $P<0.01$ ) and P2ry6 (A\_64\_P042495; FC=7.37;  $P<0.05$ ) were among the first 20 upregulated mRNAs (Tables IV and V and Fig. 5). Dlx3 was the second downregulated mRNA [FC absolute (ABS)=7.79;  $P<0.05$ ] Tables IV and V, and Fig. 5). Tp53 was among the first 20 downregulated mRNAs [FC (ABS)=5.01,  $P<0.01$ ] (Tables IV and V and Fig. 5).

*Adamts7 and P2ry6 proteins are differentially expressed in endometriosis, but not Dlx3 and Tp53.* Validation was performed using samples from 13 rats in the endometriosis group, eight in the adipose tissue control group and 14 in the blank control group. Fig. 6A shows that Adamts7 was expressed in the uterine tissues of all three groups during the implantation stage, mainly in the endometrial stroma, glands and uterine cavity epithelium. The expression in the endometriosis group was upregulated significantly in comparison with the two control groups (adipose tissue and blank controls) in the three types of tissues ( $P<0.05$ ). The Adamts7 expression was significantly increased in the adipose tissue control group compared with in the blank control group in uterine stroma and glandular epithelium ( $P<0.05$ ; Fig. 6B).

P2ry6 was expressed in the uterine tissues of all three groups of rats during the implantation stage, mainly in the endometrial stroma, glands and uterine cavity epithelium. The expression of P2ry6 was significantly increased in the endometriosis group compared with in the two control groups in the three tissue types ( $P<0.05$ ). The expression of P2ry6 was also significantly increased in the adipose tissue control

group compared with in the blank control group in uterine epithelium and stroma ( $P<0.05$ ; Fig. 6C).

Dlx3 was expressed in the uterine tissues of all three groups of rats, mainly in the endometrial stroma and uterine cavity epithelium. The expression in the glands was relatively weak. In the endometrial stroma and uterine epithelium, there was no significant difference in Dlx3 expression between the endometriosis and adipose tissue control groups ( $P=0.291$  and  $P=0.98$ ), and the expression in the endometriosis and adipose tissue control groups was significantly downregulated in comparison with the blank control group ( $P<0.05$ ). There were no significant differences in the expression of Dlx3 in the uterine glandular epithelium among the three groups ( $P=0.80$ ; Fig. 6D).

Tp53 was expressed in the uterine tissues of all three groups of rats, mainly in the endometrial stroma and uterine cavity epithelium. In all three tissue types, there was no significant difference in Tp53 expression between the endometriosis and adipose tissue control groups ( $P=0.089$ ) and the expression the endometriosis and adipose tissue control groups was significantly downregulated in comparison with the blank control group ( $P<0.05$ ; Fig. 6E).

Taken together, those results suggest that endometriosis is associated with increased protein expression of Adamts7 and P2ry6, while Dlx3 and Tp53 are not changed by endometriosis. Changes in Dlx3 and Tp53 protein expression could be due to the surgery.

*Western blot analysis.* Adamts7 was significantly upregulated in the endometriosis group in comparison with the adipose tissue control group ( $P=0.002$ ) and blank control group ( $P=0.003$ ), and its expression in the adipose tissue

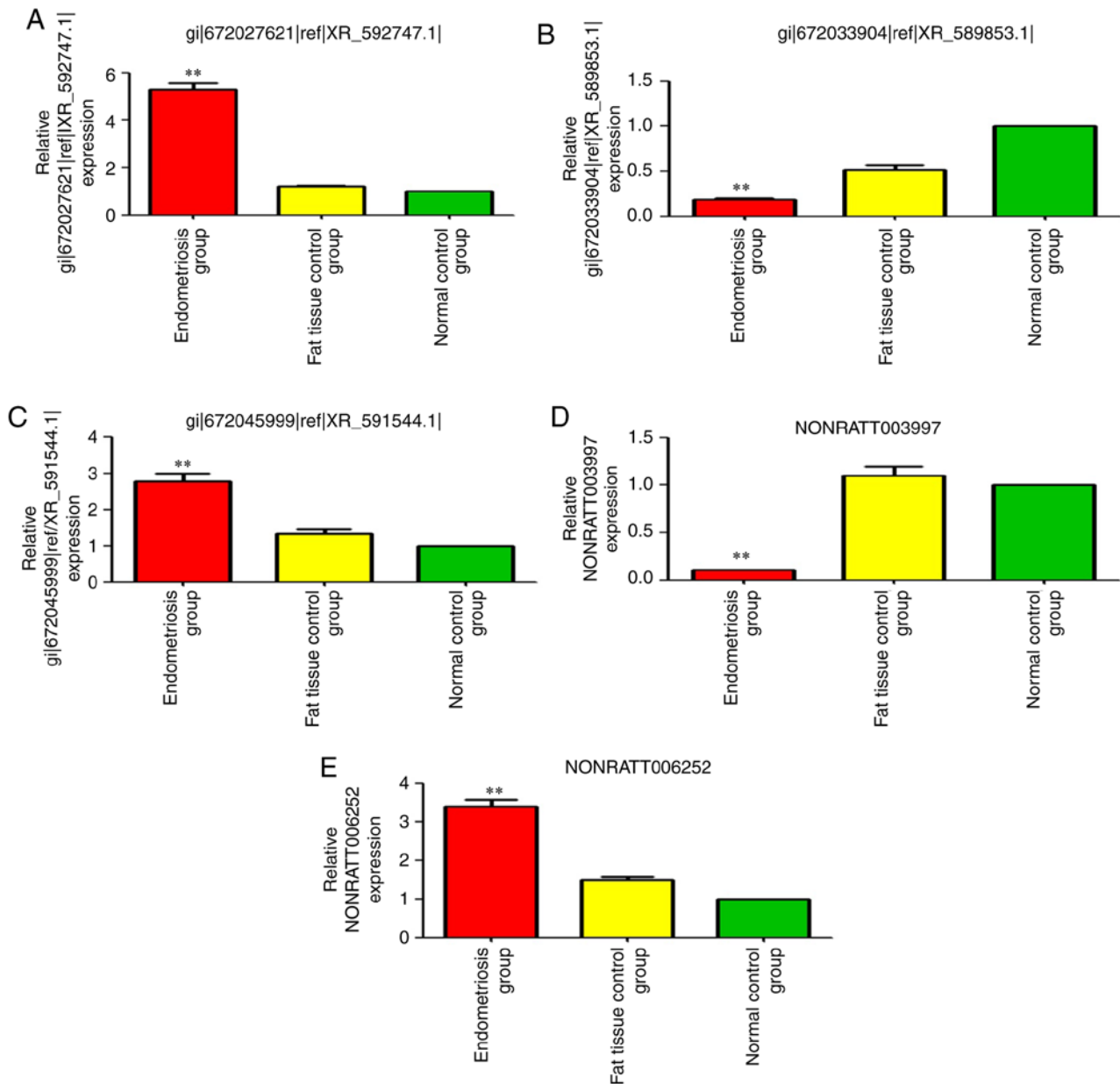


Figure 3. Changes in the expression of the five differentially expressed lncRNAs among the three groups. (A) *gil672027621|reflXR\_592747.1|*, (B) *gil672033904|reflXR\_589853.1|*, (C) *gil672045999|reflXR\_591544.1|*, (D) *NONRATT003997* and (E) *NONRATT006252*. \*\*P<0.01 vs. the normal control. lnc, long noncoding.

control group was significantly upregulated compared with the blank control group (P=0.004; Fig. 7A and B). The expression of P2ry6 in the endometriosis group was significantly upregulated compared with the adipose tissue control group (P=0.001) and blank control group (P=0.001), and its expression in the adipose tissue control group was significantly increased compared with in the blank control group (P=0.004; Fig. 7A and C). The expression of TP53 in the adipose tissue control group was significantly downregulated. compared with the blank control group (P=0.004; Fig. 7A and E). The expression of Dlx3 in the endometriosis group was significantly downregulated compared with the adipose tissue control group (P=0.002) and blank control group (P=0.002); its expression in the adipose tissue control group was significantly downregulated compared with the blank control group (P=0.002; Fig. 7A and D). Taken together, those results show that the Adamts7 and P2ry6 proteins are

upregulated by endometriosis, while Dlx3 and Tp53 are downregulated (Fig. 7).

**GO and KEGG analysis.** In the GO pathway analysis, the mRNAs that were abnormally expressed were mainly involved in cell differentiation, response to oxygen-containing compounds, ureteric bud morphogenesis, ureter maturation, embryonic organ morphogenesis, endocrine hormone secretion, female pregnancy, the immune response, response to steroid hormones, the ER-nucleus signaling pathway, parturition, response to oxidative stress, reproductive processes, response to estrogen, regulation of reproductive processes, *in utero* embryonic development and placenta development (Table VI).

In the KEGG analysis (Fig. 8), differentially expressed mRNAs were mainly involved in estrogen signaling pathway, GnRH signaling pathway, inflammatory mediator regulation of TRP channels, endometrial cancer, ovarian steroidogenesis,

Table III. Top 20 downregulated lncRNA.

lncRNA (probe name)	FC (abs)	P-value	lncRNA (name)
NONRATT003997	10.9511	0.00237	
NONRATT024485	10.62082	0.018243	
NONRATT009394	9.938666	0.044736	
gil672086757lreflXR_597443.1l	8.693425	0.014136	LOC103694443
NONRATT016350	8.277449	0.007646	
NONRATT001658	7.982786	0.002575	
NONRATT005792	6.014078	0.00994	
gil672033904lreflXR_589853.1l	5.79144	0.01007	LOC102546604
NONRATT014091	5.124274	0.014968	
gil672040874lreflXR_590738.1l	4.626765	0.018434	LOC103691378
uc.340	3.967024	0.00138	
NONRATT011360	3.901989	0.002246	
gil672030085lreflXR_598174.1l	3.857016	0.017871	LOC102553701
gil672060549lreflXR_355981.2l	3.720889	0.007524	LOC102547634
NONRATT003965	3.631949	0.001985	
gil672027547lreflXR_592687.1l	3.62932	0.002161	LOC102547023
gil672034604lreflXR_589986.1l	3.453335	0.00527	LOC103690992
NONRATT003634	3.397446	0.014216	
NONRATT018412	3.134341	0.015503	
gil672027788lreflXR_340220.2l	3.128051	0.010927	LOC102551595

lnc, long noncoding; abs, absolute.

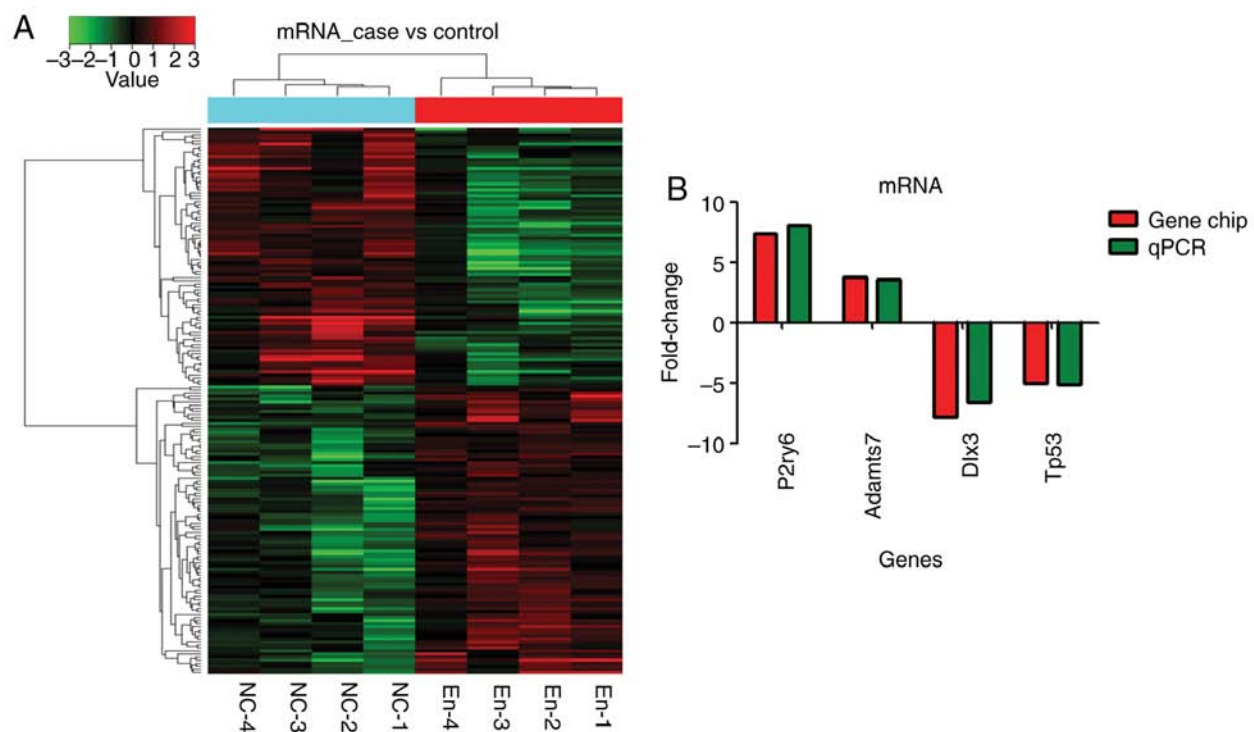


Figure 4. Compared with the blank control group (n=4), the endometriosis model group (n=4) shows that 182 mRNA transcripts were different: 97 were upregulated and 85 were downregulated (fold-change >2). (A) Gene chip analysis. (B) Reverse transcription-qPCR confirmation using four mRNAs. The samples were tested in triplicates. q, quantitative.

steroid hormone biosynthesis, apoptosis signaling pathway, insulin/IGF pathway-mitogen activated protein kinase/MAP

kinase cascade, inflammation mediated by chemokine and cytokine signaling pathway.



Table IV. Top 20 upregulated mRNA.

Probe name	mRNA	FC (abs)	P-value
A_64_P366031	Cbln1	7.464442	0.002725
A_64_P042495	P2ry6	7.37147	0.02699
A_64_P066251	Ms4a14	5.004323	0.026015
A_64_P021845	Tac3	4.34276	0.024744
A_44_P241448	LOC102550973	3.948064	0.022094
A_64_P057276	LOC102549073	3.933694	0.023946
A_42_P817214	Efcab3	3.786581	0.004338
A_44_P964460	Adamts7	3.75427	0.01493
A_44_P506980	Pou3f4	3.655452	0.008571
A_64_P044628	Agtr1b	3.09492	0.017631
A_64_P012957	Dntt	3.094423	0.014797
A_64_P016978	Zfp488	3.061541	0.003415
A_64_P087831	Galnt13	3.038959	0.005398
A_44_P135990	Cd3g	2.947655	0.002446
A_64_P071732	Lrrc4c	2.944548	0.01782
A_44_P375658	Nxph1	2.943451	0.002413
A_44_P1071620	Sit1	2.608929	0.006022
A_64_P059820	Xkr6	2.532615	0.013807
A_64_P003997	Igsf1	2.527809	0.023865
A_64_P113401	Fam183b	2.519156	0.00364

Abs, absolute.

Table V. Top 20 downregulated mRNA.

Probe name	mRNA	FC (abs)	P-value
A_64_P009530	LOC687483	8.781071	0.003707
A_44_P575055	Dlx3	7.794150	0.014970
A_64_P142988	Fosb	7.026777	0.029057
A_44_P295042	Cxcl5	6.987926	0.012344
A_64_P094855	Slc46a2	5.017081	0.002092
A_64_P121136	Tp53	5.013210	0.008090
A_43_P11576	Hspa1b	4.539404	0.024537
A_64_P043411	Elf3	4.520617	0.006673
A_42_P576446	Krt17	4.418501	0.019014
A_64_P062413	Calml3	4.182893	0.004898
A_64_P017515	Ppp1r35	3.717559	0.014440
A_64_P014090	Grp	3.703025	0.028939
A_44_P271658	LOC100912449	3.625274	0.008212
A_64_P072638	Jsrp1	3.393673	0.006873
A_64_P124621	LOC102555023	3.319351	0.006541
A_64_P135713	Mbnl3	3.274797	0.010593
A_64_P113635	RGD1563753	3.230319	0.005243
A_64_P031497	Murc	3.213777	0.013858
A_44_P107653	Lrrc26	2.927319	0.027704
A_64_P002809	Tubb4a	2.853953	0.008596

In unsupervised hierarchical clustering analysis, the differentially expressed lncRNA (Fig. 2A) and mRNA (Fig. 4A) were used to generate heat maps, and they segregated into the endometriosis group and the normal control group clusters.

**lncRNA and mRNA co-expression profiles and lncRNA function prediction.** Numerous lncRNA bind thousands of mRNA to achieve their biological functions. One lncRNA can bind to multiple mRNAs and one mRNA might be the target gene for multiple lncRNAs. For example, as shown in this study, Dlx3 was targeted by 32 lncRNA, TP53 was targeted by 35 lncRNA, P2ry6 was targeted by 33 lncRNA, Adamts7 was targeted by 40 lncRNA, NONRATT003997 targeted 21 mRNA, gil672027621|reflXR\_592747.1| targeted 23 mRNA, gil672045999|reflXR\_591544.1| targeted 29 mRNA, NONRATT006252 targeted 24 mRNA, and gil672033904|reflXR\_589853.1| targeted 32 mRNA (Tables VI and V). Taken together, these results indicate that the effect of endometriosis on uterine lncRNA and mRNA is complex (Table VII and Fig. 9).

## Discussion

The present study showed that there were 115 upregulated lncRNAs, 51 downregulated lncRNAs, 97 upregulated mRNAs and 85 downregulated mRNAs in the uterine tissues of rats with endometriosis, compared with the control group. The relative protein expression levels of Adamts7, P2ry6, Dlx3 and TP53 were different in the endometriosis group. Bioinformatics could predict the co-expression relationship of

the selected five lncRNAs and four mRNAs. GO and KEGG analyses predicted that Adamts7, P2ry6, Dlx3, and TP53 were involved in endometriosis-related inflammation and reproductive pathways. Taken together, the results strongly suggest that the changes in the expression of lncRNAs, mRNAs and Adamts7, P2ry6, Dlx3 and TP53 proteins may possibly affect endometrial receptivity in rats with endometriosis during the implantation window.

Wang *et al* (7) found that the co-expression relationship of lncRNA(HOX)A11-AS1 (HOXA11 antisense RNA) and homeobox A (HOXA9, HOXA10, HOXA11 and HOXA13) played an important role in the pathogenesis of abdominal wall endometriosis. Powell *et al* (22) served the association among the allele 1p36.12 of LINC00339, blood CDC42 and endometriosis. Sun *et al* (9) found that 948 lncRNA transcripts and 4,088 mRNA transcripts were abnormally expressed in the ectopic endometrium of patients with endometriosis using gene chip technology. Ghazal *et al* (5) confirmed that H19 acted as a molecular sponge and attenuated the bioactivity of let-7 in the eutopic endometrium of patients with endometriosis; the expression of H19 in the endometrium of patients with endometriosis was significantly downregulated compared with those without endometriosis. Sigurgeirsson *et al* (23) found that the expression of 3,297 mRNAs, 516 lncRNAs and 102 small non-coding RNAs in the endometrium were significantly different between the proliferative phase and secretory phase of women's normal menstrual cycle (7-9 days after ovulation), and they speculated that the changes in the expression level of lncRNAs and mRNAs were probably the reasons for impaired endometrial receptivity. Shin *et al* (24) found that in the four-cell stage of embryo development in

Table VI. GO analysis of mRNA.

Term	ID	Background number	P-value
Reproduction	GO:0000003	715	0.934613717
Steroid metabolic process	GO:0008202	205	0.907802417
Embryo development ending in birth or egg hatching	GO:0009792	519	0.907802417
Sexual reproduction	GO:0019953	543	0.828851221
Placenta development	GO:0001890	127	0.809271211
Steroid biosynthetic process	GO:0006694	115	0.785775079
Embryonic epithelial tube formation	GO:0001838	105	0.767818727
<i>In utero</i> embryonic development	GO:0001701	321	0.720657678
Regulation of hormone secretion	GO:0046883	196	0.706512715
Blastocyst development	GO:0001824	66	0.655993287
Embryonic heart tube development	GO:0035050	64	0.648745020
Maternal process involved in female pregnancy	GO:0060135	59	0.632235095
Embryo development	GO:0009790	780	0.605305219
Response to estrogen	GO:0043627	231	0.572555551
Multicellular organismal reproductive behavior	GO:0033057	25	0.453156618
Hormone transport	GO:0009914	253	0.437730680
Chronic inflammatory response	GO:0002544	22	0.432311123
Regulation of inflammatory response to antigenic stimulus	GO:0002861	20	0.411517366
Parturition	GO:0007567	17	0.389834482
Uterus development	GO:0060065	16	0.383439641

GO, gene ontology.

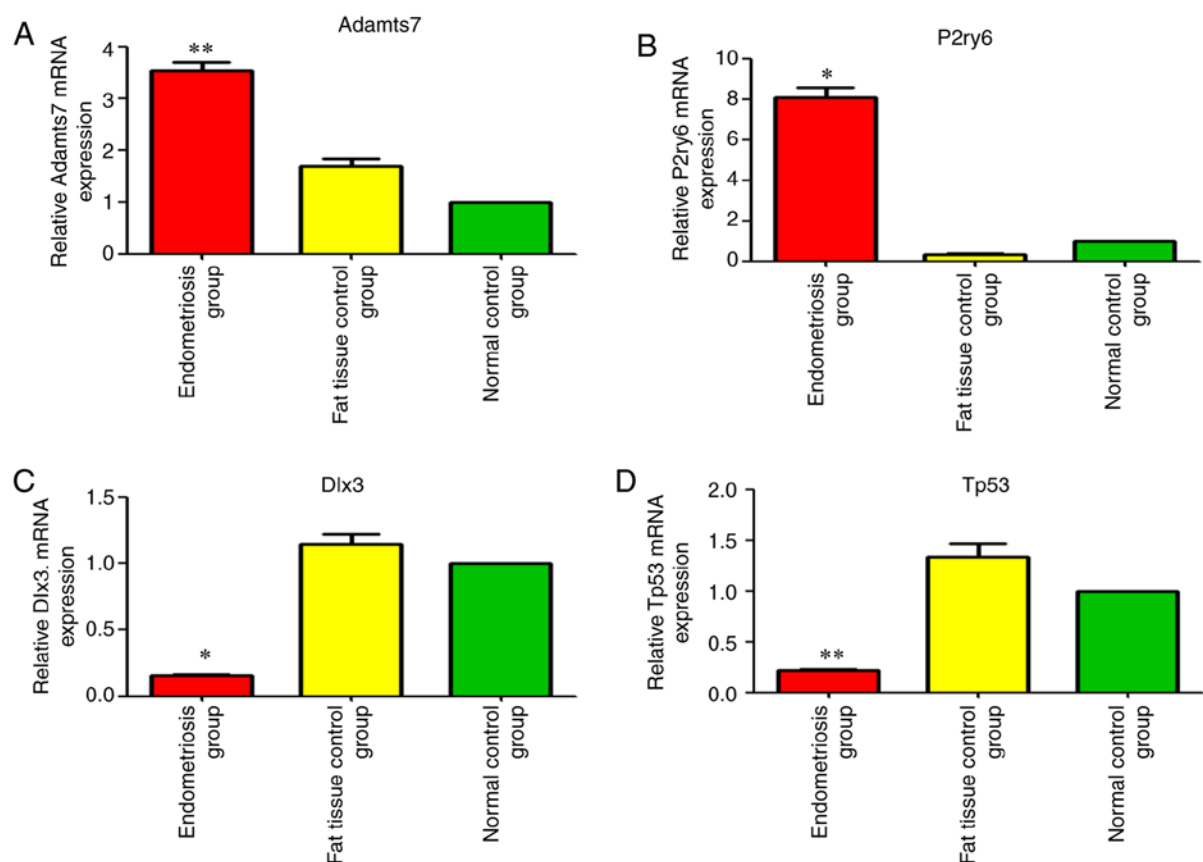


Figure 5. Changes in the expression of the four differentially expressed mRNAs among the three groups. mRNA expression of (A) Adamts7, (B) P2ry6 (C) Dlx3 and (D) Tp53. \* $P < 0.05$  and \*\* $P < 0.01$  vs. the normal control. Adamts7, ADAM metalloproteinase with thrombospondin type 1 motif 7; Tp53, tumor protein p53; Dlx3, distal-less homeobox 3; P2ry6, pyrimidinergic receptor P2Y6.

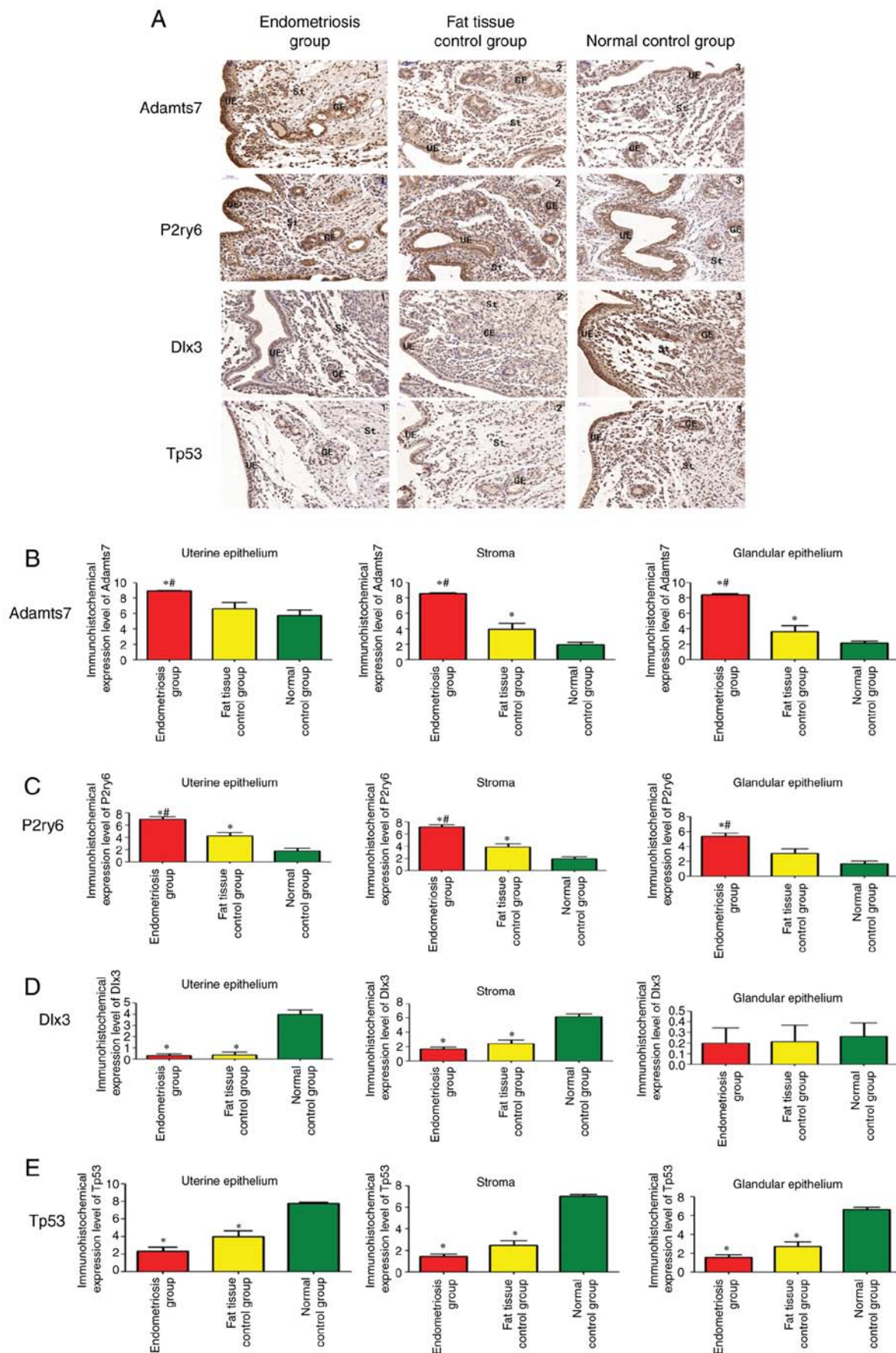


Figure 6. Immunohistochemistry of uterine tissue in rats. (A) Expression of Adams7, P2ry6, Dlx3 and Tp53 in the endometriosis group (n=13), adipose tissue control group (n=8) and blank control group (n=14). (magnification, x200). Quantification of the immunohistochemistry results for (B) Adams7, (C) P2ry6, (D) Dlx3 and (E) Tp53. The samples were tested in triplicates. \*P<0.05 vs. blank controls. <sup>#</sup>P<0.05 vs. adipose tissue controls. Adams7, ADAM metalloproteinase with thrombospondin type 1 motif 7; Tp53, tumor protein p53; Dlx3, distal-less homeobox 3; P2ry6, pyrimidinergic receptor P2Y6; GE, glandular epithelium; St, endometrial stroma; UE, uterine epithelium.

Table VII. Expression of lncRNA and mRNA.

Source	Target	Correlation	P-value	Source gene symbol	Target gene symbol
gil672033904 reflXR_589853.1l	A_64_P135713	0.992091	0.000001	gil672033904	Dlx3
NONRATT003997	A_64_P135713	0.928748	0.000857	-	Dlx3
gil672027621 reflXR_592747.1l	A_64_P135713	-0.92396	0.001037	gil672027621	Dlx3
gil672033904 reflXR_589853.1l	A_64_P113635	0.961171	0.000142	gil672033904	Tp53
NONRATT003997	A_64_P113635	0.96782	0.000081	-	Tp53
gil672045999 reflXR_591544.1l	A_64_P113635	-0.91168	0.00161	gil672045999	Tp53
NONRATT006252	A_42_P814235	0.957719	0.000183	-	P2ry6
gil672027621 reflXR_592747.1l	A_42_P814235	0.919696	0.001218	gil672027621	P2ry6
gil672045999 reflXR_591544.1l	A_42_P814235	0.919036	0.001248	gil672045999	P2ry6
gil672033904 reflXR_589853.1l	A_44_P178519	-0.95751	0.000186	gil672033904	Adamts7
NONRATT006252	A_44_P178519	0.912129	0.001586	-	Adamts7
NONRATT003997	A_44_P178519	-0.9136	0.00151	-	Adamts7
gil672027621 reflXR_592747.1l	A_44_P178519	0.921091	0.001157	gil672027621	Adamts7
gil672045999 reflXR_591544.1l	A_44_P178519	0.944424	0.000411	gil672045999	Adamts7

lnc, long noncoding; Adamts7, ADAM metalloproteinase with thrombospondin type 1 motif 7; Tp53, tumor protein p53; Dlx3, distal-less homeobox 3; P2ry6, pyrimidinergic receptor P2Y6.

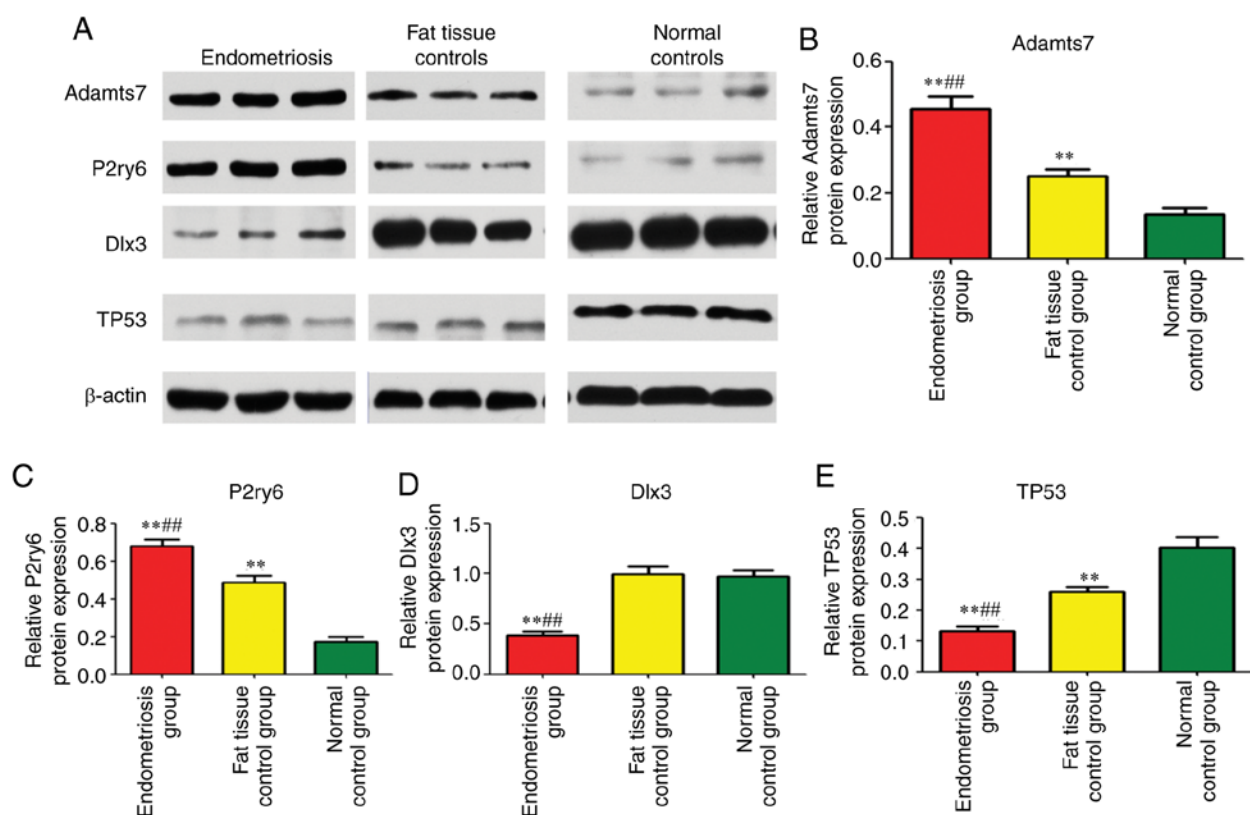


Figure 7. Western blot analysis of uterine tissue in rats. (A) Expression of Adamts7, P2ry6, Dlx3 and Tp53 in the endometriosis group (n=13), adipose tissue control group (n=8) and blank control group (n=14). Quantification of the western blotting results for (B) Adamts7, (C) P2ry6, (D) Dlx3 and (E) Tp53. The samples were tested in triplicates.  $\beta$ -actin was used to normalize the data. \*\* $P$ <0.01 vs. normal control, \*\*\* $P$ <0.01 vs. adipose tissue controls. Adamts7, ADAM metalloproteinase with thrombospondin type 1 motif 7; Tp53, tumor protein p53; Dlx3, distal-less homeobox 3; P2ry6, pyrimidinergic receptor P2Y6.

female rats, the X chromosome was selectively silenced and inactivated; during this process, lncRNA Xist was activated by the downregulation of ubiquitin ligase Rnf12/RLIM3-5 in the embryonic cells. It has been shown that lncRNAs play a key

role in human embryo implantation (25). In the present study, a rat endometriosis model was established by mating to obtain uterine tissues during the implantation window. This study is the first study to the best of our knowledge on the expression



Table VIII. Comparison between rat and human lncRNA sequences.

Rat lncRNA	Human lncRNA	% identical	lncRNA ID
gil672027621reflXR_592747.11	p17451	90.31	TCONS_00001579
NONRATT022454	p44032_v4	83.45	uc001cvx.3
gil672045999reflXR_591544.11	p10107	83.29	ENST00000563759.1
NONRATT014258	RNA40309 RefSeq_2352_1430	90.06	
NONRATT011779	RNA38792 RefSeq_733_3290	81.9	
NONRATT029450	RNA42607 UCSC_176_6901	100	
NONRATT028550	p28817	86.47	LIT3372
NONRATT003997	p37546_v4	84.17	ENST00000514073.1
NONRATT027560	p28817	81.42	LIT3372
NONRATT000719	RNA45098 UCSC_3204_2521	88	
NONRATT017840	RNA43455 UCSC_1198_3829	81.71	

lnc, long noncoding.

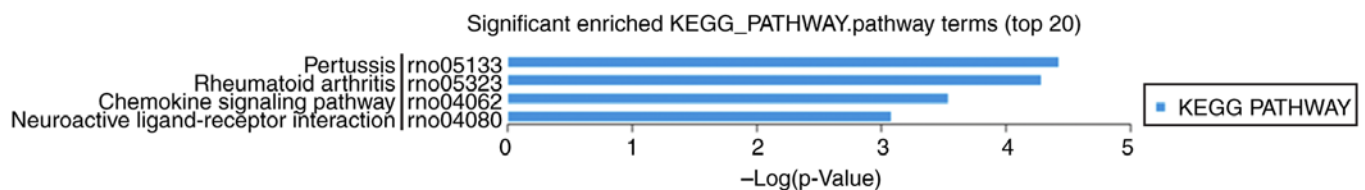


Figure 8. KEGG analysis of differentially expressed lncRNAs. lnc, long noncoding; KEGG, Kyoto Encyclopedia of Genes and Genomes.

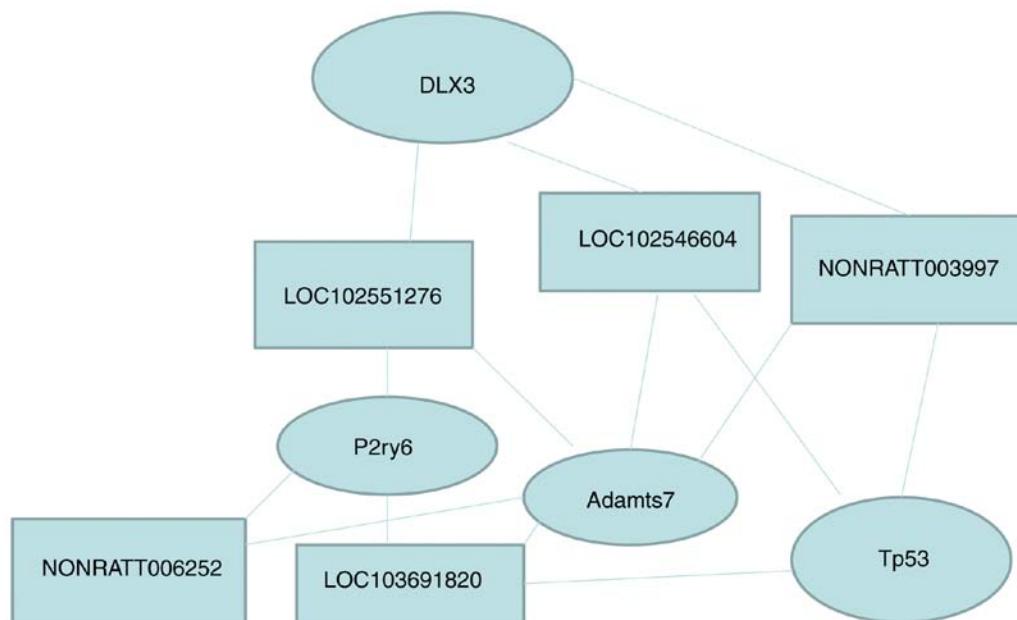


Figure 9. Relationships among the five differentially expressed lncRNAs and the four mRNAs. The lncRNAs and mRNA shown here are those that were validated by quantitative PCR. The samples were tested in triplicates. lnc, long noncoding; Adams7, ADAM metalloproteinase with thrombospondin type 1 motif 7; Tp53, tumor protein p53; Dlx3, distal-less homeobox 3; P2ry6, pyrimidinergic receptor P2Y6.

profile of lncRNA and mRNA in endometriosis during the implantation window.

Adams7 belongs to a group of proteins that have platelet-associated activity (26). The overexpression of ADAMTS-7 promotes the decomposition of cartilage

oligomeric matrix protein and accelerates the development of osteoarthritis induced by surgery and collagen-induced arthritis (27). In the present study, Adams7 was mainly expressed in the endometrial stroma, glands and uterine cavity epithelium, the expression in the uterine tissues of rats with



endometriosis was upregulated, and the expression in the adipose tissue control group was also upregulated in comparison with that of the blank control group. Therefore, it could be hypothesized that implantation failure in endometriosis during the implantation stage could be related to inflammation and the function of secretory glands.

Giannattasio *et al* (28) showed that as a G-protein combined receptor and a uridine diphosphate receptor, P2ry6 has a high affinity for G-protein combined receptor and uridine-2-phosphate receptor, which is an important endogenous inhibitor of the function of T cells in allergic pulmonary inflammation. Hamby *et al* (29) showed that transforming growth factor- $\beta$ 1, lipopolysaccharide, interferon- $\gamma$  and other inflammatory factors can cause immune injury in astrocytes through the expression of P2ry6, leading to nervous system dysfunction. In the present study, the expression of P2ry6 in the uterine tissues of rats with endometriosis was upregulated during the implantation stage and the expression in the operation control group was upregulated in comparison with that of the blank control group. Therefore, this study considered that the gene regulation of P2ry6 in rats with endometriosis during the implantation window might be related to inflammation and hormone levels, which needs to be confirmed.

Dlx3 has been widely studied in the course of pregnancy and plays an important role in the formation of the placenta (30-32). DLX3 is expressed in the placenta tissues during human early pregnancy and plays an important regulatory role in the trophoblastic layer, syncytial layer and the formation of primary villi (33). Berghorn *et al* (34) showed that DLX3 in the placental tissues of 8.5-day mouse embryonic development was not detected, but DLX3 could be detected at 9.5 days and continued to 15.5 days. DLX3 produces  $\beta$ -hydroxysteroid dehydrogenase (VI) during the process of the secretion of progesterone by placental trophoblast cells and the expression of DLX3 is not detected in the embryonic stem cells (Rcho-1) of rats (34). In the present study, the expression of DLX3 in the endometrial stroma in rats with endometriosis during the implantation window was not significantly different from that of the operation control group and they were both decreased compared with in the blank control group. It was hypothesized that the effect of DLX3 on rats with endometriosis during the implantation window was mainly reflected in the endometrial stroma, which might not be related to gland activity and hormone levels, but more closely related to inflammation. Nevertheless, changes in the expression of DLX3 could be due to the surgery (35). Additional studies are necessary to examine this.

Tp53 acts as a bridge in the exchange process of pregnant mother and fetus in the early stages. The inactivation of Tp53 is affected by the preimplantation factor and may cause the apoptosis of placental cells, indicating that the interaction of Tp53 and implantation factors in human placental cytotrophoblasts promotes the survival and growth of embryonic cells (36). The expression profile of TP53 fluctuates during pregnancy (37). In human placental cells, adiponectin induces caspase activity by increasing the expression of TP53 and BAX, leading to a decrease in the expression of adiponectin receptors, and affecting the nutrient transport function of the placenta (38). Tp53 was also a downregulated gene in the uterine tissues of rats with endometriosis during the implantation window, but there was no significant difference between the endometriosis group and

operation control group, both of them showing downregulated levels in comparison with those of the blank control group. Tp53 probably plays an important role in the formation of endometrial receptivity in rats with endometriosis during the implantation window, which might be related to the endometriosis-associated inflammatory characteristics and gland secretion. As for DLX3, changes in Tp53 could also be due to surgery (39). This will have to be examined in the future.

The present study is not without limitations. Although the present study could efficiently avoid the effects of the menstrual cycle in different individuals, it was still impossible to avoid the disadvantages of using animal experiments. There were also some differences among animals and the endometrium could not be separated because the uterine tissues of rats are too small. Therefore, the gene expression profile in the uterine tissues was decreased compared with the endometrium. Moreover, although human lncRNA sequence are highly similar to rats', there are still some differences (Table VIII). Therefore, the next step will be to compare the degree of conservation of human and rat lncRNA sequences. On the basis of the obtained gene data of lncRNA and mRNA expression profiles in the uterine tissues of rats with endometriosis during the implantation window, five lncRNAs were compared with the conservative sequence of the human lncRNA database, showing that the lncRNAs were highly consistent. The correlation analyses indicate a relationship among the lncRNAs and mRNAs, but not the exact causal nature of the relationships. Finally, no functional and mechanistic experiments were performed to confirm the GO and KEGG results. Additional studies are still necessary to confirm the roles of the differentially expressed lncRNAs and mRNAs identified in the present study.

The results showed that the changes in the expression of lncRNAs, mRNAs and proteins (Adamts7, P2ry6, Dlx3 and TP53) may possibly affect the endometrial receptivity in rats with endometriosis during the implantation window, probably resulting in implantation failure of the embryo. This study provides new insights to investigate the pathogenesis of the disease and new clues about the possible causes of implantation failure in patients with endometriosis. It could ultimately reveal treatment targets for endometriosis infertility, but RNA stability is still a major barrier to the successful development of RNA therapeutics.

## Acknowledgements

Not applicable.

## Funding

No funding was received.

## Availability of data and materials

All data generated or analyzed during this study are included in this published article.

## Authors' contributions

HC conceived and coordinated the study, designed, performed and analyzed the experiments, wrote the paper. XZ, ZL, YZ,

JL carried out the data collection, data analysis, and revised the paper. All authors reviewed the results and approved the final version of the manuscript.

### Ethics approval and consent to participate

This study was approved by the experimental animal center of Peking Union Medical College Hospital and Chinese Academy of Medical Sciences (permit no. XHDW-2016-000). All experiments were performed in accordance with the principles of experimental animal management and protection. The rats were humanely sacrificed as necessary to prevent suffering.

### Patient consent for publication

Not applicable.

### Competing interests

All authors declare that they have no competing interests.

### References

- Bedaiwy MA, Alfaraj S, Yong P and Casper R: New developments in the medical treatment of endometriosis. *Fertil Steril* 107: 555-565, 2017.
- Zhao Y, Gong P, Chen Y, Nwachukwu JC, Srinivasan S, Ko C, Bagchi MK, Taylor RN, Korach KS, Nettles KW, *et al*: Dual suppression of estrogenic and inflammatory activities for targeting of endometriosis. *Sci Transl Med* 7: 271ra9, 2015.
- de Ziegler D, Pirtea P, Galliano D, Cicinelli E and Meldrum D: Optimal uterine anatomy and physiology necessary for normal implantation and placentation. *Fertil Steril* 105: 844-854, 2016.
- Lessey BA and Kim JJ: Endometrial receptivity in the eutopic endometrium of women with endometriosis: It is affected, and let me show you why. *Fertil Steril* 108: 19-27, 2017.
- Ghazal S, McKinnon B, Zhou J, Mueller M, Men Y, Yang L, Mueller M, Flannery C, Huang Y and Taylor HS: H19 lncRNA alters stromal cell growth via IGF signaling in the endometrium of women with endometriosis. *EMBO Mol Med* 7: 996-1003, 2015.
- Liang Z, Chen Y, Zhao Y, Xu C, Zhang A, Zhang Q, Wang D, He J, Hua W and Duan P: miR-200c suppresses endometriosis by targeting MALAT1 in vitro and in vivo. *Stem Cell Res Ther* 8: 251, 2017.
- Wang M, Hao C, Huang X, Bao H, Qu Q, Liu Z, Dai H, He S and Yan W: Aberrant expression of lncRNA (HOXA11-AS1) and homeobox A (HOXA9, HOXA10, HOXA11, and HOXA13) genes in infertile women with endometriosis. *Reprod Sci* 25: 654-661, 2018.
- Sha L, Huang L, Luo X, Bao J, Gao L, Pan Q, Guo M, Zheng F and Wang H: Long non-coding RNA LINC00261 inhibits cell growth and migration in endometriosis. *J Obstet Gynaecol Res* 43: 1563-1569, 2017.
- Sun PR, Jia SZ, Lin H, Leng JH and Lang JH: Genome-wide profiling of long noncoding ribonucleic acid expression patterns in ovarian endometriosis by microarray. *Fertil Steril* 101: 1038-1046 e7, 2014.
- Rekker K, Saare M, Eriste E, Tasa T, Kukuškina V, Roost AM, Anderson K, Samuel K, Karro H, Salumets A and Peters M: High-throughput mRNA sequencing of stromal cells from endometriomas and endometrium. *Reproduction* 154: 93-100, 2017.
- Wang Y, Li Y, Yang Z, Liu K and Wang D: Genome-wide microarray analysis of long non-coding RNAs in eutopic secretory endometrium with endometriosis. *Cell Physiol Biochem* 37: 2231-2245, 2015.
- Vernon MW and Wilson EA: Studies on the surgical induction of endometriosis in the rat. *Fertil Steril* 44: 684-694, 1985.
- Keenan JA, Williams-Boyce PK, Massey PJ, Chen TT, Caudle MR and Bukovsky A: Regression of endometrial explants in a rat model of endometriosis treated with the immune modulators loxoribine and levamisole. *Fertil Steril* 72: 135-141, 1999.
- Cai H, Zhu XX, Li ZF, Zhu YP and Lang JH: MicroRNA dysregulation and steroid hormone receptor expression in uterine tissues of rats with endometriosis during the implantation window. *Chin Med J (Engl)* 131: 2193-2204, 2018.
- Makrigiannakis A, Zoumakis E, Kalantaridou S, Coutifaris C, Margioris AN, Coukos G, Rice KC, Gravanis A and Chrousos GP: Corticotropin-releasing hormone promotes blastocyst implantation and early maternal tolerance. *Nat Immunol* 2: 1018-1024, 2001.
- Xiao L, Wu J, Wang JY, Chung HK, Kalakonda S, Rao JN, Gorospe M and Wang JY: Long noncoding RNA uc.173 promotes renewal of the intestinal mucosa by inducing degradation of microRNA 195. *Gastroenterology* 154: 599-611, 2018.
- Livak KJ and Schmittgen TD: Analysis of relative gene expression data using real-time quantitative PCR and the 2(-Delta Delta C(T)) method. *Methods* 25: 402-408, 2001.
- Konno R, Yamakawa H, Utsunomiya H, Ito K, Sato S and Yajima A: Expression of survivin and Bcl-2 in the normal human endometrium. *Mol Hum Reprod* 6: 529-534, 2000.
- Guttman M, Amit I, Garber M, French C, Lin MF, Feldser D, Huarte M, Zuk O, Carey BW, Cassady JP, *et al*: Chromatin signature reveals over a thousand highly conserved large non-coding RNAs in mammals. *Nature* 458: 223-227, 2009.
- Wong ES, Schmitt BM, Kazachenka A, Thybert D, Redmond A, Connor F, Rayner TF, Feig C, Ferguson-Smith AC, Marioni JC, *et al*: Interplay of cis and trans mechanisms driving transcription factor binding and gene expression evolution. *Nat Commun* 8: 1092, 2017.
- Wang Q, Wang N, Cai R, Zhao F, Xiong Y, Li X, Wang A, Lin P and Jin Y: Genome-wide analysis and functional prediction of long non-coding RNAs in mouse uterus during the implantation window. *Oncotarget* 8: 84360-84372, 2017.
- Powell JE, Fung JN, Shakhbazov K, Sapkota Y, Cloonan N, Hemani G, Hillman KM, Kaufmann S, Luong HT, Bowdler L, *et al*: Endometriosis risk alleles at 1p36.12 act through inverse regulation of CDC42 and LINC00339. *Hum Mol Genet* 25: 5046-5058, 2016.
- Sigurgeirsson B, Amark H, Jemt A, Ujvari D, Westgren M, Lundeberg J and Gidlöf S: Comprehensive RNA sequencing of healthy human endometrium at two time points of the menstrual cycle. *Biol Reprod* 96: 24-33, 2017.
- Shin J, Wallingford MC, Gallant J, Marcho C, Jiao B, Byron M, Bossenz M, Lawrence JB, Jones SN, Mager J and Bach I: RLIM is dispensable for X-chromosome inactivation in the mouse embryonic epiblast. *Nature* 511: 86-89, 2014.
- Bouckenheimer J, Assou S, Riquier S, Hou C, Philippe N, Sansac C, Lavabre-Bertrand T, Combes T, Lemaître JM, Boureux A and De Vos J: Long non-coding RNAs in human early embryonic development and their potential in ART. *Hum Reprod Update* 23: 19-40, 2016.
- Liu CJ: The role of ADAMTS-7 and ADAMTS-12 in the pathogenesis of arthritis. *Nat Clin Pract Rheumatol* 5: 38-45, 2009.
- Zhang Y, Wei F and Liu CJ: Overexpression of ADAMTS-7 leads to accelerated initiation and progression of collagen-induced arthritis in mice. *Mol Cell Biochem* 404: 171-179, 2015.
- Giannattasio G, Ohta S, Boyce JR, Xing W, Balestrieri B and Boyce JA: The purinergic G protein-coupled receptor 6 inhibits effector T cell activation in allergic pulmonary inflammation. *J Immunol* 187: 1486-1495, 2011.
- Hamby ME, Coppola G, Ao Y, Geschwind DH, Khakh BS and Sofroniew MV: Inflammatory mediators alter the astrocyte transcriptome and calcium signaling elicited by multiple G-protein-coupled receptors. *J Neurosci* 32: 14489-14510, 2012.
- King JH, Kwan STC, Yan J, Klatt KC, Jiang X, Roberson MS and Caudill MA: Maternal choline supplementation alters fetal growth patterns in a mouse model of placental insufficiency. *Nutrients* 9: E765, 2017.
- Murthi P, Hiden U, Rajaraman G, Liu H, Borg AJ, Coombes F, Desoye G, Brennecke SP and Kalionis B: Novel homeobox genes are differentially expressed in placental microvascular endothelial cells compared with macrovascular cells. *Placenta* 29: 624-630, 2008.
- Clark PA, Brown JL, Li S, Woods AK, Han L, Sones JL, Preston RL, Southard TL, Davison RL and Roberson MS: Distal-less 3 haploinsufficiency results in elevated placental oxidative stress and altered fetal growth kinetics in the mouse. *Placenta* 33: 830-838, 2012.
- Chui A, Pathirage NA, Johnson B, Cocquebert M, Fournier T, Evain-Brion D, Roald B, Manuelpillai U, Brennecke SP, Kalionis B and Murthi P: Homeobox gene distal-less 3 is expressed in proliferating and differentiating cells of the human placenta. *Placenta* 31: 691-697, 2010.

34. Berghorn KA, Clark PA, Encarnacion B, Deregis CJ, Folger JK, Morasso MI, Soares MJ, Wolfe MW and Roberson MS: Developmental expression of the homeobox protein distal-less 3 and its relationship to progesterone production in mouse placenta. *J Endocrinol* 186: 315-323, 2005.
35. Zhan Y, Li X, Gou X, Yuan G, Fan M and Yang G: DLX3 inhibits the proliferation of human dental pulp cells through inactivation of canonical Wnt/ $\beta$ -catenin signaling pathway. *Front Physiol* 9: 1637, 2018.
36. Moindjie H, Santos ED, Gouesse RJ, Swierkowski-Blanchard N, Serazin V, Barnea ER, Vialard F and Dieudonné MN: Preimplantation factor is an anti-apoptotic effector in human trophoblasts involving p53 signaling pathway. *Cell Death Dis* 7: e2504, 2016.
37. Kaczmarek MM, Krawczynski K, Najmala J, Reliszko ZP, Sikora M and Gajewski Z: Differential expression of genes linked to the leukemia inhibitor factor signaling pathway during the estrus cycle and early pregnancy in the porcine endometrium. *Reprod Biol* 14: 293-297, 2014.
38. Duval F, Santos ED, Poidatz D, Serazin V, Gronier H, Vialard F and Dieudonné MN: Adiponectin inhibits nutrient transporters and promotes apoptosis in human villous cytotrophoblasts: Involvement in the control of fetal growth. *Biol Reprod* 94: 111, 2016.
39. Hausmann R, Nerlich A and Betz P: The time-related expression of p53 protein in human skin wounds-a quantitative immunohistochemical analysis. *Int J Legal Med* 111: 169-172, 1998.



This work is licensed under a Creative Commons Attribution-NonCommercial-NoDerivatives 4.0 International (CC BY-NC-ND 4.0) License.